Available online at http://scik.org
J. Math. Comput. Sci. 2023, 13:8
https://doi.org/10.28919/jmcs/8038
ISSN: 1927-5307

STABILITY ANALYSES ON THE EFFECT OF VACCINATION AND CONTACT TRACING IN MONKEYPOX VIRUS TRANSMISSION

SOLOMON ESHUN[1,*], RICHMOND ESSIEKU[1,2], JAMES LADZEKPO[3]

[1]School of Mathematical and Statistical Sciences, University of Texas Rio Grande Valley, Edinburg, TX, USA

[2]Department of Economics, Texas Tech University, Lubbock, TX, USA

[3]Department of Mathematics, Western Michigan University, Kalamazoo, MI, USA

Abstract. Monkeypox is a significant health concern due to its potential for morbidity and occasional mortality. Vaccination and effective contact tracing play pivotal roles in controlling infectious diseases, including monkeypox. This study aims to contribute to our understanding of monkeypox dynamics by developing a comprehensive mathematical model that incorporates key factors such as vaccination, quarantining, and contact tracing. Through rigorous sensitivity analysis, we explore the impact of varying vaccination coverage and contact tracing on the disease's dynamics. In particular, we investigate the dynamics of the disease in relation to variable vaccination coverage and contact tracing. Our findings highlight the critical role of vaccination and contact tracing in reducing monkeypox transmission. Higher vaccination coverage, combined with effective contact tracing and other control measures, leads to increased stability of the disease-free equilibrium and a decreased likelihood of sustained outbreaks. These findings emphasize the need for continued efforts in promoting vaccination programs and strengthening contact tracing capabilities to effectively manage and contain monkeypox transmissions.

Keywords: monkeypox; vaccination; contact tracing; sensitivity analysis; control measures.

2020 AMS Subject Classification: 92C60.

*Corresponding author

E-mail address: solomon.eshun01@utrgv.edu

Received May 30, 2023

1. INTRODUCTION

Monkeypox is a contagious disease that can be transmitted between animals and humans. It is similar to smallpox and has been a significant worry for a long time. It was initially identified in monkeys at the State Serum Institute in Copenhagen, Denmark, in 1958 [1]. This marked the first known instance of the disease being observed in monkeys. Since then, outbreaks have occurred in humans, primarily in Central and West Africa, specifically in countries like Nigeria, Cameroon, Liberia and Sierra Leone [2, 3].

Throughout history, outbreaks of monkeypox have been documented in different primate species, exhibiting distinct skin eruptions and lesions. However, in the 1970s, it became evident that the virus could also infect humans, leading to concerns as it emerged in areas where smallpox had already been eliminated. The transmission dynamics of the virus include zoonotic transmission from animals, human and potentially environmental factors [4].

Monkeypox virus primarily spreads to humans from wild animals like rodents and primates, and human-to-human transmission is also common. The transmission among humans is associated with respiratory droplets, contact with bodily fluids, contaminated environments or items, and direct contact with skin lesions of infected individuals [5]. Since the eradication of smallpox, monkeypox virus has become the most prevalent orthopoxvirus [6]. Its infection manifests with symptoms typically appearing 7 to 14 days (incubation period) after exposure, as noted in a study by Emeka et al. [7]. Common symptoms include fever, headache, swollen lymph nodes, chills and fatigue. These manifestations are often experienced by individuals who have contracted the disease. Although monkeypox has a lower fatality rate compared to smallpox, it can still cause significant harm, particularly among vulnerable populations. Furthermore, the absence of a specific treatment or vaccine for monkeypox poses additional challenges in containing and preventing its transmission. With the rise in monkeypox cases in recent years, there is an urgent requirement to investigate and comprehend its transmission dynamics.

Mathematical modeling has emerged as a valuable approach in understanding infectious diseases and devising effective control measures. It has a number of benefits since it enables researchers to model and examine the complex dynamics of disease transmission while taking into account a range of variables like population demographics, disease traits, and treatment options.

This offers a methodical and quantitative approach for investigating the effect and transmission of diseases. Also, mathematical models make it possible to explore many situations and do "what-if" evaluations, which can help with decision-making and direct the creation of the best control plans. Researchers can evaluate the potential efficacy of various control strategies and prioritize resource allocation by modifying model parameters and evaluating alternative intervention scenarios.

In the past, monkeypox has received limited attention, resulting in a lack of comprehensive understanding regarding its transmission mechanisms. The quest to understand the mechanism of monkeypox has been a subject of extensive research to date. A significant number of research have focused in particular on developing models to explain the transmission dynamics. Notably, Bhunu and Mushayabasa [2] conducted a transmission analysis of monkeypox virus, serving as a valuable resource for understanding the dynamics of pox-like diseases. Another study by Usman and Adamu [8] focused on examining the dynamics of monkeypox virus in human hosts and rodents, along with stability analysis. Furthermore, significant contributions can be found in studies by Olumuyiwa et al. [4], Madubueze et al. [9], Bankuru et al. [10], and Grant et al. [11]. Collectively, these studies have advanced our understanding of monkeypox and its transmission dynamics.

It has a number of benefits since it enables researchers to model and examine the intricate dynamics of illness transmission while taking into account a range of variables like population demographics, disease traits, and treatment options. This offers a methodical and quantitative approach for investigating the effect and transmission of illnesses.

While the existing research is limited, a few mathematical models have been developed to investigate monkeypox transmission, with a specific emphasis on quarantine and vaccination strategies. The success of vaccination in eradicating smallpox has led to the recognition of its potential in controlling closely related orthopoxviruses, including monkeypox. Furthermore, the implementation of quarantine measures has proven effective in mitigating the spread of infectious diseases by reducing contact between infected individuals and susceptible populations [9]. This highlights the necessity for in-depth research and the application of control strategies to effectively control the transmission of monkeypox.

As a result, our study aims to conduct sensitivity analyses to examine the impact of crucial parameters, including vaccination coverage, transmission probability and effective contact tracing, on the control of monkeypox. This analysis will provide insights into the significance of these factors in shaping the dynamics of the disease transmission and offer valuable information for the development of strategies to prevent and control the disease. By investigating the stability and sensitivity of monkeypox transmission in relation to vaccination and quarantine interventions, our research will contribute to the expanding knowledge on effective measures against monkeypox.

2. MODEL FORMULATION

A comprehensive understanding of the disease under consideration is crucial in developing a mathematical model for the disease. Additionally, during the formulation of the model, it is essential to recognize that as the infection disseminates among the population, the population is divided into distinct compartments that do not overlap. The constructed mathematical model should effectively depict the dynamics of each compartment, considering how they evolve over time, as described by Madubueze et al. [9].

Drawing inspiration from the fundamental concept and framework of mathematical modeling in epidemiology [12], our model encompasses the dynamics of ten distinct sub-populations. Specifically, we consider susceptible (S_h), exposed (E_h), vaccinated (V_h), quarantined (Q_h), infected (I_h), treated (T_h), and recovered (R_h) individuals within the human population. Additionally, the model incorporates susceptible (S_r), exposed (E_r), and infected (I_r) individuals within the rodent population.

The total human population at time t, denoted as $N_h(t)$, is the sum of the individual human sub-populations:

$$N_h(t) = S_h(t) + V_h(t) + E_h(t) + Q_h(t) + I_h(t) + T_h(t) + R_h(t) \tag{1}$$

Likewise, the total rodent population at time t, denoted as $N_r(t)$, is calculated by summing the corresponding sub-populations:

$$N_r(t) = S_r(t) + E_r(t) + I_r(t) \tag{2}$$

The entry of susceptible individuals into the human population is facilitated by immigration or birth, with a constant rate denoted as Π. The susceptible human population, decreases due to vaccination at a rate π, while it increases through the loss of vaccine-acquired immunity among vaccinated individuals at a waning rate χ. As a result, a vaccinated human who loses immunity becomes susceptible with no vaccine protection. The transmission of monkeypox infection to susceptible humans occurs through effective contact with either infectious rodents or infectious humans. The force of infection, denoted as λ_h, measures the probability of susceptible humans contracting monkeypox infection upon exposure to infectious rodents or infectious humans. It represents the combined impact of both infectious rodents and infectious humans in transmitting the virus to susceptible humans, and it is defined by Equation 3.

$$\bar{\lambda}_h = \frac{\theta_r I_r(t) + \theta_h I_h(t)}{N_h(t)} \tag{3}$$

where θ_h and θ_r are transmission probability from infectious humans to susceptible humans and infectious rodents to susceptible humans respectively.

The population of exposed humans consists of susceptible individuals who contract the virus at a rate $\bar{\lambda}_h$. Subsequently, some of these individuals transition to the quarantine compartments at a rate η, as a result of contact tracing and quarantine measures implemented after the incubation period. Quarantine aims to isolate exposed individuals and prevent further virus transmission. For the exposed individuals who do not enter $Q_h(t)$, a proportion of β progresses to the infected class, representing the rate at which they become capable of transmitting the virus. Once individuals enter $I_h(t)$, they become infectious and can transmit monkeypox to susceptible individuals. The infected human population also experiences an additional death rate, δ, which accounts for the potential mortality associated with monkeypox infection. Individuals in the quarantined and infected classes will enter the treatment class at a rate of ϕ and α respectively, after obvious symptoms appear and they are diagnosed eventually. Fraction of the treated individuals recover and progress to the recovered class at a rate of ρ.

For the rodents population, the susceptible rodents class, $S_r(t)$, is recruited at a constant rate Λ, and is decreased through acquiring infection following substantial contact with infectious

rodents at a rate $\bar{\lambda}_r$, defined by Equation 4.

$$\bar{\lambda}_r = \frac{\theta I_r(t)}{N_r(t)} \tag{4}$$

where, θ is the transmission probability from infectious rodents to susceptible rodents.

The population of exposed rodents, denoted as $E_r(t)$, is formed through interactions between susceptible rodents and infected rodents. Within this population, a proportion of κ subsequently transitions to the infected rodent class, signifying the rate at which susceptible rodents become infected.

It is important to note that both the human and rodent populations experience a homogeneous natural death rate. For the human population, this rate is denoted as μ_h, while for the rodent population, it is denoted as μ_r.

The entire transmission dynamics is depicted in Figure 1 below.

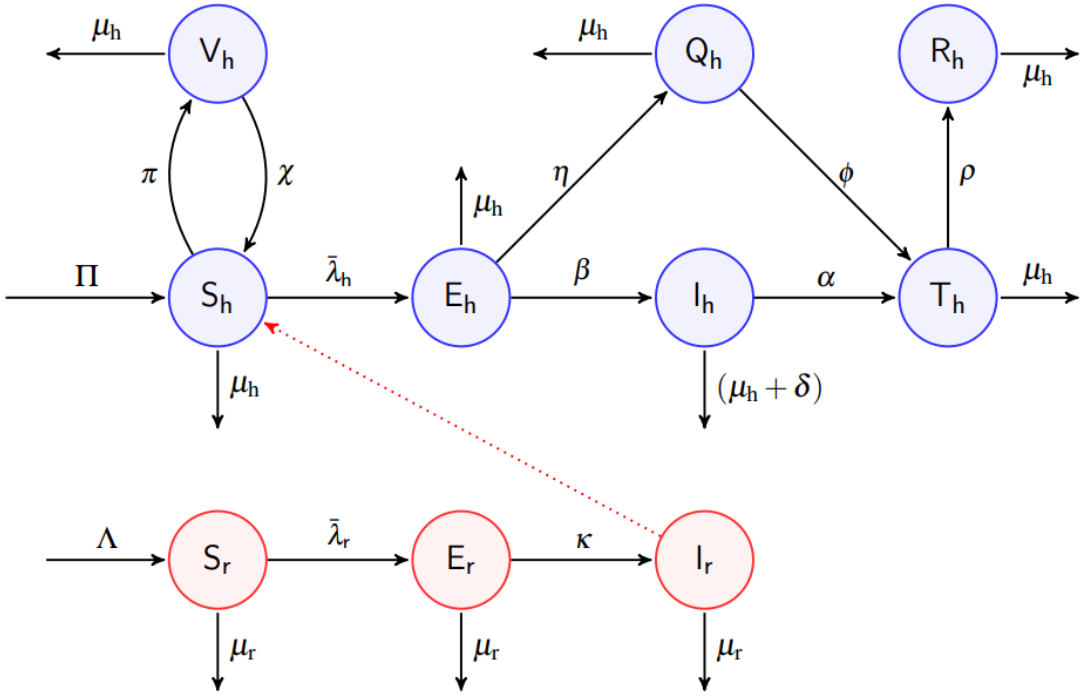

FIGURE 1. Flow diagram for monkeypox transmission dynamics with control measures

Table 1 presents a comprehensive overview of the parameters in the model. Building upon the model description, we derive the system of differential equations as follows:

$$
\begin{cases}
\dfrac{\mathrm{d}S_h}{\mathrm{d}t} = \Pi + \chi V_h - (\bar{\lambda}_h + \pi + \mu_h) S_h \\
\dfrac{\mathrm{d}V_h}{\mathrm{d}t} = \pi S_h - (\chi + \mu_h) V_h \\
\dfrac{\mathrm{d}E_h}{\mathrm{d}t} = \bar{\lambda}_h S_h - (\beta + \eta + \mu_h) E_h \\
\dfrac{\mathrm{d}Q_h}{\mathrm{d}t} = \eta E_h - (\phi + \mu_h) Q_h \\
\dfrac{\mathrm{d}I_h}{\mathrm{d}t} = \beta E_h - (\alpha + \delta + \mu_h) I_h \\
\dfrac{\mathrm{d}T_h}{\mathrm{d}t} = \alpha I_h + \phi Q_h - (\rho + \mu_h) T_h \\
\dfrac{\mathrm{d}R_h}{\mathrm{d}t} = \rho T_h - \mu_h R_h \\
\dfrac{\mathrm{d}S_r}{\mathrm{d}t} = \Lambda - (\bar{\lambda}_r + \mu_r) S_r \\
\dfrac{\mathrm{d}E_r}{\mathrm{d}t} = \bar{\lambda}_r S_r - (\kappa + \mu_r) E_r \\
\dfrac{\mathrm{d}I_r}{\mathrm{d}t} = \kappa E_r - \mu_r I_r
\end{cases}
\tag{5}
$$

It is assumed that all the model parameters are non-negative.

TABLE 1. Description of Model Parameters

Parameter	Description	Value	Reference
Π	Recruitment rate into susceptible human population	0.029	[2]
Λ	Recruitment rate into susceptible rodent population	0.020	[2]
π	Proportion of vaccinated humans	0.1-1	Varied
χ	Proportion of unsuccessful vaccinated humans	0.1-1	Varied
ϕ	Treatment rate of quarantined humans	0.3	Assumed
β	Proportion of exposed human to infected state	0.2	[9]
α	Treatment rate of infected humans	0.2	Assumed
ρ	Recovery rate of infected humans due to treatment	0.83	[2]
κ	Proportion of exposed rodents to infected rodents	0.3	[8]
θ	Rodent-to-rodent transmission probability	0.0027	[2]
θ_r	Rodent-to-human transmission probability	0.00025	[2]
θ_h	Human-to-human transmission probability	0.00006	[2]
δ	Monkeypox-induced death rate of humans	0.2	[4]
η	Proportion of effective contact tracing for exposed humans	0.1-1	Varied
μ_{r}	Natural death rate of rodents	0.3	[9]
μ_h	Natural death rate of humans	0.2	[9]

3. MODEL ANALYSIS

In this section, we performed a quantitative analysis to investigate the key properties of the model. Specifically, we focused on examining the feasibility of the system and ensuring the positivity of its solutions. The model system described by equation 5 was studied within a biologically feasible region, denoted as Ω, which can be further divided into two regions: $\Omega = \Omega_h \times \Omega_r$.

3.1. Boundedness of the Model. The system described by the model in 5 is considered to be well-posed and meaningful when its global solution remains within a positive invariant region. This region is characterized by non-negative variables and parameters for all time $t \geq 0$ [13]. This condition ensures that the variables and parameters involved in the model have realistic interpretations and maintain non-negative values throughout the dynamics of the system. The

concept of a positive invariant region provides confidence in the validity and significance of the model's implications, as it guarantees the system's behavior aligns with the expected properties of the studied phenomenon.

Theorem 3.1. *The solution set* $\{S_h, V_h, E_h, Q_h, I_h, T_h, R_h, S_r, E_r, I_r\} \in \mathbb{R}_+^{10}$ *of the model system 5 is contained in the feasible region* Ω.

Proof: Under non-negative initial conditions, the model system described by 5 has a single non-negative solution for all time $t \geq 0$, which remains within a specific region. By following the methods proposed by Asamoah et al. [13] Busenberg and Cooke[14] and Stuart and Humphries[15], we differentiate Equations 1 and 2 to achieve the following results.

$$\frac{\mathrm{d}N_h}{\mathrm{d}t} = -\mu_h N_h - \delta I_h + \Pi \tag{6}$$

$$\frac{\mathrm{d}N_r}{\mathrm{d}t} = -\mu_r N_r + \Lambda \tag{7}$$

Now, assuming that there is no monkeypox-induced death rate in the infected human compartment, it implies that 6 becomes

$$\frac{\mathrm{d}N_h}{\mathrm{d}t} = -\mu_h N_h + \Pi \tag{8}$$

Suppose that $dN_h/dt \leq 0$, $dN_r/dt \leq 0$, $N_h \leq \Pi/\mu_h$ and $N_r \leq \Lambda/\mu_r$, and then imposing the theorem used in [13] on differential inequality results in $0 \leq N_h \leq \Pi/\mu_h$ and $0 \leq N_r \leq \Lambda\mu_r$. Therefore, Equations 7 and 8 becomes

$$\frac{\mathrm{d}N_h}{\mathrm{d}t} \leq -\mu_h N_h + \Pi \tag{9}$$

$$\frac{\mathrm{d}N_r}{\mathrm{d}t} \leq -\mu_r N_r + \Lambda \tag{10}$$

Solve 9 and 10 using the integrating factor method. After some algebraic manipulation the feasible solution of the rodents and human population in model system 5 is in the region

$$\Omega = \left\{ (S_h, V_h, E_h, Q_h, I_h, T_h, R_h) \in \mathbb{R}_+^7 : N_h \leq \frac{\Pi}{\mu_h},\ (S_r, E_r, I_r) \in \mathbb{R}_+^3 : N_r \leq \frac{\Lambda}{\mu_r} \right\} \tag{11}$$

Therefore, the feasible solutions are contained in Ω. Hence the human population size $N_h \to \Pi/\mu_h$ as $t \to \infty$. Similarly, the total rodents population size $N_r \to \Lambda/\mu_r$ as $t \to \infty$. This means that the infected state variables of the two populations tend to zero as time goes to infinity.

Therefore, the region Ω is attracting all the solutions in $\mathbb{R}^{10}_{+}$. Hence, the model is mathematically well posed and epidemiologically meaningful.

3.2. Positivity of the Solutions. We demonstrate that all the state variables in the mathematical model of monkeypox transmission dynamics remain non-negative for all $t > 0$. This indicates that the model has epidemiological significance and is mathematically well-defined. We present and provide a proof for the following theorem:

Theorem 3.2. *Given the initial conditions* $\{S_{h0}, V_{h0}, E_{h0}, Q_{h0}, I_{h0}, T_{h0}, R_{h0}, S_{r0}, E_{r0}, I_{r0} \geq 0\} \in \mathbb{R}^{10}_{+}$. *Then the solution set for the model in 5,* $\{S_h, V_h, E_h, Q_h, I_h, T_h, R_h, S_r, E_r, I_r\}$ *are positive for all* $t \geq 0$.

Proof: Using the approach of Chinwendu et al. [9], it follows from the first equation of the system that

$$\frac{\mathrm{d}S_h}{\mathrm{d}t} = \Pi + \chi V_h - (\bar{\lambda}_h + \pi + \mu_h)S_h$$

$$\implies \frac{\mathrm{d}S_h}{\mathrm{d}t} \geq -(\bar{\lambda}_h + \pi + \mu_h)S_h \tag{12}$$

Using the method of separation of variables to simplify further, we have

$$S_h \geq Ce^{-(\bar{\lambda}_h + \pi + \mu_h)t} \tag{13}$$

From the initial condition, we have that

$$S_h \geq S_{h0}e^{-(\bar{\lambda}_h + \pi + \mu_h)t} \tag{14}$$

which is positive, given that S_{h0} is also positive.

Similarly, this can be demonstrated for the remaining state variables in the model. This observation is supported by the fact that exponential functions and initial solutions are non-negative. Thus, the solution set remains non-negative for all time periods $t \geq 0$.

4. Equilibrium Points and Basic Reproduction Number

4.1. Disease-Free Equilibrium Point. The disease-free equilibrium, DFE refers to a state in which the population remains free from the disease. Mathematically, DFE is obtained by setting all equations of the model to zero and substituting the corresponding values of the state

variables. Let $E_0 = \left(S_h^0, V_h^0, E_h^0, Q_h^0, I_h^0, T_h^0, R_h^0, S_r^0, E_r^0, I_r^0\right)$ be the disease-free equilibrium of 5. For the developed model, we have

$$E_0 = \left(\frac{\Pi(\pi+\mu_{\mathrm{h}})}{\mu_{\mathrm{h}}(\chi+\pi+\mu_{\mathrm{h}})}, \frac{\Pi\pi}{\mu_{\mathrm{h}}(\chi+\pi+\mu_{\mathrm{h}})}, 0, 0, 0, 0, 0, \frac{\Lambda}{\mu_{\mathrm{r}}}, 0, 0\right) \tag{15}$$

4.2. Basic Reproduction Number. In infectious disease epidemiology, the basic reproduction number, $\mathfrak{R}_0$, is arguably a significant threshold. It is the main determinant of whether a possible outbreak of a disease can generate into an epidemic or not. $\mathfrak{R}_0$ can be thought of as the average number of new cases of infection caused by one normal infected individual in a completely susceptible population [16]. It helps to determine the stability of the disease-free and endemic equilibrium points in the model.

The computation of $\mathfrak{R}_0$ in this study follows the approach proposed by Diekmann et al. [16]. This method involves considering the rates of new infection (f_i) and transitional terms (v_i) in each compartment of the model. By applying this approach to the monkeypox model, described by 5, we obtain the next-generation matrix as follows:

$$f_i = \begin{pmatrix} \frac{(\theta_h I_h + \theta_r I_r)\mu_h S_h}{\Pi} \\ 0 \\ 0 \\ \frac{\theta\mu_r \theta I_r S_r}{\Lambda} \\ 0 \end{pmatrix} \quad \text{and} \quad v_i = \begin{pmatrix} (\beta+\eta+\mu_h)E_h \\ -\beta E_h + (\alpha+\delta+\mu_h)I_h \\ -\alpha Q_h + (\rho+\mu_h)T_h \\ (\kappa+\mu_r)E_r \\ -\kappa E_r + \mu_r I_r \end{pmatrix} \tag{16}$$

Taking partial derivatives of equation 16 with respect to E_h, I_h, T_h, E_r and I_r and evaluating at E_0 gives:

(17)

$$F = \begin{pmatrix} 0 & \frac{\theta_h\mu_h S_h^0}{\Pi} & 0 & 0 & \frac{\theta_r\mu_h S_h^0}{\Pi} \\ 0 & 0 & 0 & 0 & 0 \\ 0 & 0 & 0 & 0 & 0 \\ 0 & 0 & 0 & 0 & \frac{\theta\mu_r S_r^0}{\Lambda} \\ 0 & 0 & 0 & 0 & 0 \end{pmatrix} \quad \text{and} \quad V = \begin{pmatrix} \beta+\eta+\mu_h & 0 & 0 & 0 & 0 \\ -\beta & \alpha+\delta+\mu_h & 0 & 0 & 0 \\ 0 & 0 & \rho+\mu_h & 0 & 0 \\ 0 & 0 & 0 & \kappa+\mu_r & 0 \\ 0 & 0 & 0 & -\kappa & \mu_r \end{pmatrix}$$

Hence, we evaluate FV^{-1} at the disease-free equilibrium as:

$$FV^{-1} = \begin{pmatrix} \frac{\theta_h \beta Z}{(\alpha+\delta+\mu_h)(\beta+\eta+\mu_h)} & \frac{\theta_h Z}{(\alpha+\delta+\mu_h)} & 0 & 0 & \frac{\theta_r Z}{\mu_r} \\ 0 & 0 & 0 & 0 & 0 \\ 0 & 0 & 0 & 0 & 0 \\ 0 & 0 & 0 & \frac{\theta\kappa}{\mu_r(\kappa+\mu_r)} & \frac{\theta}{\mu_r} \\ 0 & 0 & 0 & 0 & 0 \end{pmatrix} \tag{18}$$

where, $Z = (\chi+\mu_h)/(\chi+\pi+\mu_h)$.

$\mathfrak{R}_0$ is calculated as the spectral radius of the matrix FV^{-1}. The eigenvalues of FV^{-1} are determined, and the value of $\mathfrak{R}_0$ is obtained as the maximum among the set $\{0,0,0,\mathfrak{R}_{0h},\mathfrak{R}_{0r}\}$. Here, $\mathfrak{R}_{0h}$ and $\mathfrak{R}_{0r}$ are defined in Equation 19. This definition allows us to assess the potential for disease transmission: if $\mathfrak{R}_0 < 1$, the infection can be eliminated in both human and rodent populations, while $\mathfrak{R}_0 > 1$ indicates the potential for persistence of the infection in both host populations.

$$\mathfrak{R}_{0h} = \frac{\theta_h \beta\,(\chi+\mu_h)}{(\chi+\pi+\mu_h)\,(\beta+\eta+\mu_h)\,(\alpha+\delta+\mu_h)} \quad \text{and} \quad \mathfrak{R}_{0r} = \frac{\theta\kappa}{\mu_r\,(\kappa+\mu_r)} \tag{19}$$

$\mathfrak{R}_{0h}$ and $\mathfrak{R}_{0r}$ are the reproduction numbers for human-to-human transmission and rodent-to-rodent transmission respectively.

4.3. Existence of Endemic Equilibrium Point. The endemic equilibrium point is a state in which the disease remains prevalent within the population. It is characterized by the values of $\left(S_h^*, V_h^*, E_h^*, Q_h^*, I_h^*, T_h^*, R_h^*, S_r^*, E_r^*, I_r^*\right)$. Thus, we can express the endemic equilibrium as follows:

(20)

$$
\begin{cases}
S_h^* = \dfrac{\Pi(\chi+\mu_h)}{{\mu_h}^2+\left(\pi+\chi+\lambda_h^*\right)\mu_h+\chi\,\lambda_h^*} \\
V_h^* = \dfrac{\Pi\pi}{{\mu_h}^2+\left(\pi+\chi+\lambda_h^*\right)\mu_h+\chi\,\lambda_h^*} \\
E_h^* = \dfrac{\lambda_h^*\,\Pi\,(\mu_h+\chi)}{(\beta+\eta+\mu_h)\left({\mu_h}^2+\left(\pi+\chi+\lambda_h^*\right)\mu_h+\chi\,\lambda_h^*\right)} \\
Q_h^* = \dfrac{\eta\Pi\lambda_h^*\,(\mu_h+\chi)}{(\beta+\eta+\mu_h)\,(\phi+\mu_h)\left({\mu_h}^2+\left(\pi+\chi+\lambda_h^*\right)\mu_h+\chi\,\lambda_h^*\right)} \\
I_h^* = \dfrac{\lambda_h^*\,\Pi\,(\mu_h+\chi)\,\beta}{(\alpha+\delta+\mu_h)\,(\beta+\eta+\mu_h)\left({\mu_h}^2+\left(\pi+\chi+\lambda_h^*\right)\mu_h+\chi\,\lambda_h^*\right)} \\
T_h^* = \dfrac{(\chi+\mu_h)\,((\alpha\,\beta+\eta\,\phi)\,\mu_h+\phi\,((\eta+\beta)\,\alpha+\eta\,\delta))\,\lambda_h^*\Pi}{(\beta+\eta+\mu_h)\,(\phi+\mu_h)\,(\alpha+\delta+\mu_h)\,(\rho+\mu_h)\left({\mu_h}^2+\left(\pi+\chi+\lambda_h^*\right)\mu_h+\chi\,\lambda_h^*\right)} \\
R_h^* = \dfrac{\rho\,(\chi+\mu_h)\,((\alpha\,\beta+\eta\,\phi)\,\mu_h+\phi\,((\eta+\beta)\,\alpha+\eta\,\delta))\,\lambda_h^*\Pi}{(\beta+\eta+\mu_h)\,(\phi+\mu_h)\,(\alpha+\delta+\mu_h)\,(\rho+\mu_h)\,\mu_h\left({\mu_h}^2+\left(\pi+\chi+\lambda_h^*\right)\mu_h+\chi\,\lambda_h^*\right)} \\
S_r^* = \dfrac{\Lambda}{\lambda_r^*+\mu_r} \\
E_r^* = \dfrac{\lambda_r^*\Lambda}{(\lambda_r^*+\mu_r)\,(\kappa+\mu_r)} \\
I_r^* = \dfrac{\kappa\,\lambda_r^*\Lambda}{\mu_r\,(\lambda_r^*+\mu_r)\,(\kappa+\mu_r)}
\end{cases}
$$

5. Stability Analysis Of The Model

5.1. Local Stability of the Disease-Free Equilibrium.

Theorem 5.1. *The disease-free equilibrium point, E_0, of the model system is locally asymptotically stable if $\mathfrak{R}_0 < 1$ and unstable otherwise.*

Proof. The Jacobian matrix, $\mathbb{J}$ of the system evaluated at E_0 is given as

(21)
$$\mathbb{J}=\begin{pmatrix}
-\mu-\pi & \chi & 0 & 0 & -\theta_h Z & 0 & 0 & 0 & 0 & -\theta_r Z \\
\pi & -\chi-\mu_h & 0 & 0 & 0 & 0 & 0 & 0 & 0 & 0 \\
0 & 0 & -\eta-\beta-\mu_h & 0 & \theta_h Z & 0 & 0 & 0 & 0 & \theta_r Z \\
0 & 0 & \eta & -\phi-\mu_h & 0 & 0 & 0 & 0 & 0 & 0 \\
0 & 0 & \beta & 0 & -\alpha-\delta-\mu_h & 0 & 0 & 0 & 0 & 0 \\
0 & 0 & 0 & \phi & \alpha & -\rho-\mu_h & 0 & 0 & 0 & 0 \\
0 & 0 & 0 & 0 & 0 & \rho & -\mu_h & 0 & 0 & 0 \\
0 & 0 & 0 & 0 & 0 & 0 & 0 & -\mu_r & 0 & -\theta \\
0 & 0 & 0 & 0 & 0 & 0 & 0 & 0 & -\kappa-\mu_r & \theta \\
0 & 0 & 0 & 0 & 0 & 0 & 0 & 0 & \kappa & -\mu_r
\end{pmatrix}$$

The eigenvalues of $\mathbb{J}$ are:

$\lambda_1=-\mu_r$, $\lambda_2=-(\chi+\pi+\mu_h)$, $\lambda_{3,4}=-\mu_h$,
$\lambda_5=-\dfrac{\kappa+2\mu_r+\sqrt{\kappa(\kappa+4\theta)}}{2}$, $\lambda_6=-\dfrac{\kappa+2\mu_r-\sqrt{\kappa(\kappa+4\theta)}}{2}$,
$\lambda_7=-\dfrac{(\eta+\beta+\alpha+\delta+2\mu_h)K+\sqrt{K((\eta+\beta-\alpha-\delta)^2K+4\beta\,\theta_h(\chi+\mu_h))}}{2K}$ and
$\lambda_8=-\dfrac{(\eta+\beta+\alpha+\delta+2\mu_h)K-\sqrt{K((\eta+\beta-\alpha-\delta)^2K+4\beta\,\theta_h(\chi+\mu_h))}}{2K}$

where, $K=(\chi+\pi+\mu_h)$.

Clearly, all the eigenvalues of the Jacobian matrix are strictly negative, provided that λ_6 and λ_8 are both negative. As a result, we seek to examine whether λ_6 and λ_8 are negative or not.

For λ_6 to be negative, we have

$$\sqrt{\kappa(\kappa+4\theta)}<\kappa+2\mu_r$$
$$\left(\sqrt{\kappa(\kappa+4\theta)}\right)^2<(\kappa+2\mu_r)^2 \tag{22}$$

Simplifying Equation 22 further gives

$$\kappa^2+4\theta\kappa<\kappa^2+4\kappa\mu_r+4\mu_r^2$$
$$\frac{4\theta\kappa}{4\mu_r(\kappa+4\mu_r)}<\frac{4\mu_r(\kappa+4\mu_r)}{4\mu_r(\kappa+4\mu_r)}$$
$$\frac{\theta\kappa}{\mu_r(\kappa+\mu_r)}<1\implies\mathfrak{R}_{0r}<1 \tag{23}$$

Therefore, λ_6 is negative when $\mathfrak{R}_{0r}<1$.

For λ_8 to be negative, it implies

$$\sqrt{K((\eta+\beta-\alpha-\delta)^2K+4\,\theta_h\beta\,(\chi+\mu_h))} < (\eta+\beta+\alpha+\delta+2\,\mu_h)\,K$$

$$K((\eta+\beta-\alpha-\delta)^2K+4\,\theta_h\beta\,(\chi+\mu_h)) < (\eta+\beta+\alpha+\delta+2\,\mu_h)^2\,K^2$$

$$4\theta_h\beta\,(\chi+\mu_h) < (\eta+\beta+\alpha+\delta+2\,\mu_h)^2\,K-(\eta+\beta-\alpha-\delta)^2K$$

$$\frac{4\theta_h\beta(\chi+\mu_h)}{4K\,(\beta+\eta+\mu_h)\,(\alpha+\delta+\mu_h)} < \frac{4K\,(\beta+\eta+\mu_h)\,(\alpha+\delta+\mu_h)}{4K\,(\beta+\eta+\mu_h)\,(\alpha+\delta+\mu_h)} \tag{24}$$

Substituting the expression of K into Equation 24, we have

$$\frac{\theta_h\beta(\chi+\mu_h)}{(\chi+\pi+\mu_h)\,(\beta+\eta+\mu_h)\,(\alpha+\delta+\mu_h)} < 1 \implies \mathfrak{R}_{0h} < 1 \tag{25}$$

Therefore, λ_8 is negative when $\mathfrak{R}_{0h} < 1$.

Therefore, the eigenvalues of $\mathbb{J}$ are all negative if $\mathfrak{R}_{0h} < 1$ and $\mathfrak{R}_{0r} < 1$. Hence, the disease-free equilibrium is locally asymptotically stable.

5.2. Global Stability of the Disease-Free Equilibrium. The global asymptotic stability of the model is examined using the approach presented by Castillo-Chavez, Feng, and Huang [17]. As a result, we rewrite the system in the form

$$\begin{cases} X'(t) = F(X,Y) \\ Y'(t) = G(X,Y), \;\; G(X,0) = 0 \end{cases} \tag{26}$$

where, $X = (S_h, V_h, R_h, S_r)$ and $Y = (E_h, Q_h, I_h, T_h, E_r, I_r)$ with $X \in \mathbb{R}^4_+$ denoting (its components) the number of uninfected individuals and $Y \in \mathbb{R}^6_+$ denoting (its components) the number of infected individuals. The disease free equilibrium is now denoted by $E_0 = (X^*, 0)$.

Theorem 5.2. *The Disease-Free Equilibrium is said to be globally asymptotically stable if* $\mathfrak{R}_0 < 1$ *and the following two conditions hold:*

C1. $X'(t) = F(X,0)$, X^* *is globally asymptotically stable.*

C2. $G(X,Y) = AY - \hat{G}(X,Y)$ *with* $\hat{G}(X,Y) \geq 0$ *for all* $(X,Y) \in \Omega$, *where* $A = G_Y(X^*,0)$.

Proof.

C1: From 5, it follows that:

(27)
$$F(X,0) = \begin{pmatrix} \Pi + \chi V_h - (\pi + \mu_h) S_h \\ \pi S_h - (\chi + \mu_h) V_h \\ -\mu_h R_h \\ \Lambda - \mu_r S_r \end{pmatrix} \implies \mathbb{J}_{F(X,0)} = \begin{pmatrix} -\pi - \mu_h & \chi & 0 & 0 \\ \pi & -\chi - \mu_h & 0 & 0 \\ 0 & 0 & -\mu_h & 0 \\ 0 & 0 & 0 & -\mu_r \end{pmatrix}$$

The system described in Equation 27 is globally asymptotically stable if all the eigenvalues of the Jacobian matrix, denoted as $\mathbb{J}_{F(X,0)}$, are negative real roots. Specifically, the eigenvalues are $-\mu_r$, $-(\chi + \pi + \mu_h)$, and $-\mu_h$ (with a multiplicity of 2). Therefore, the system exhibits global asymptotic stability due to the negativity of these eigenvalues.

C2: Since A is the partial derivative of the function $G(X,Y)$ with respect to Y at the disease-free equilibrium, we have

(28)
$$A = \begin{pmatrix} -(\beta + \eta + \mu_h) & 0 & \frac{\theta_h S_h^0}{N_h^0} & 0 & 0 & \frac{\theta_r S_h^0}{N_h^0} \\ \eta & -(\phi + \mu_h) & 0 & 0 & 0 & 0 \\ \beta & 0 & -(\alpha + \delta + \mu_h) & 0 & 0 & 0 \\ 0 & \phi & \alpha & -(\rho + \mu_h) & 0 & 0 \\ 0 & 0 & 0 & 0 & -(\kappa + \mu_r) & \frac{\theta S_r^0}{N_r^0} \\ 0 & 0 & 0 & 0 & \kappa & -\mu_r \end{pmatrix}$$

By the condition *C2*, $\hat{G}(X,Y)$ is given by

(29)
$$\hat{G}(X,Y) = \begin{pmatrix} \frac{S_h^0(\theta_h I_h + \theta_r I_r)}{N_h^0} \left(1 - \frac{S_h}{N_h} \frac{N_h^0}{S_h^0}\right) \\ 0 \\ 0 \\ 0 \\ \theta I_r \left(1 - \frac{S_r}{N_r}\right) \\ 0 \end{pmatrix} \geq 0$$

Therefore $\hat{G}(X,Y) \geq 0$ for all $(X,Y) \in \Omega$ implying that E_0 is globally asymptotically stable.

6. Sensitivity Analysis of the Basic Reproduction Number

In modeling infectious diseases, identifying key parameters that significantly influence transmission dynamics is crucial. Sensitivity analysis plays a vital role in assessing the robustness of disease models and their predictions concerning different parameter values. Sensitivity analysis quantifies the impact of varying independent variables on a specific dependent variable, based on predefined assumptions [20]. Its goal is to understand how changes in parameter values affect the outcome of interest, providing insights into the model's responsiveness to different parameter values.

The normalized forward sensitivity index is a commonly used measure to assess the sensitivity of a variable to a particular parameter. It calculates the ratio of the relative change in the variable to the relative change in the parameter. Specifically, for the variable $\mathfrak{R}_{0h}$, which is differentiably dependent on a parameter p, the normalized forward sensitivity index is defined as:

$$S_p^{\mathfrak{R}_{0h}} = \frac{\partial \mathfrak{R}_{0h}}{\partial p} \times \frac{p}{\mathfrak{R}_{0h}} \tag{30}$$

The sensitivity indices for all the parameters in $\mathfrak{R}_{0h}$ are presented in Table 2 below. A positive sensitivity index indicates that increasing the corresponding parameter, while keeping all other parameters constant, leads to an increase in the value of $\mathfrak{R}_{0h}$. This increase in $\mathfrak{R}_{0h}$ amplifies the transmission of monkeypox. On the other hand, negative sensitivity index indicate that increasing the parameter would result in a decrease in $\mathfrak{R}_{0h}$, leading to a reduction in monkeypox transmission.

TABLE 2. Sensitivity indices of model parameters in $\mathfrak{R}_{0h}$

Parameter	Sensitivity Index
π	-0.6667
χ	$+0.3333$
μ_{h}	-0.1227
δ	-0.3333
β	$+0.4908$
η	-0.3681
α	-0.1227
θ_h	$+1.0000$

Figure 2 provides a visual representation of the parameters with their respective sensitivity indices. The results reveal that the value of $\mathfrak{R}_{0h}$ decreases as the values of the control parameters η and π increase, as indicated by their negative sensitivity indices. The vaccination rate π shows a negative index, indicating that a higher vaccination rate is associated with a decrease in $\mathfrak{R}_{0h}$. This highlights the significant role of increasing vaccination coverage in reducing monkeypox transmission. Similarly, the negative index of η, implies that an increase in contact tracing leads to a decrease in $\mathfrak{R}_{0h}$. This explains the importance of effective contact tracing strategies in limiting the spread of monkeypox. The progression rate of infected individuals into the treatment class (α) also shows that a faster progression into treatment reduces $\mathfrak{R}_{0h}$ by reducing the duration of infectiousness. Finally, the human-to-human contact rate shows the highest sensitivity index of $+1$, underscoring the importance of reducing contact with infected humans.

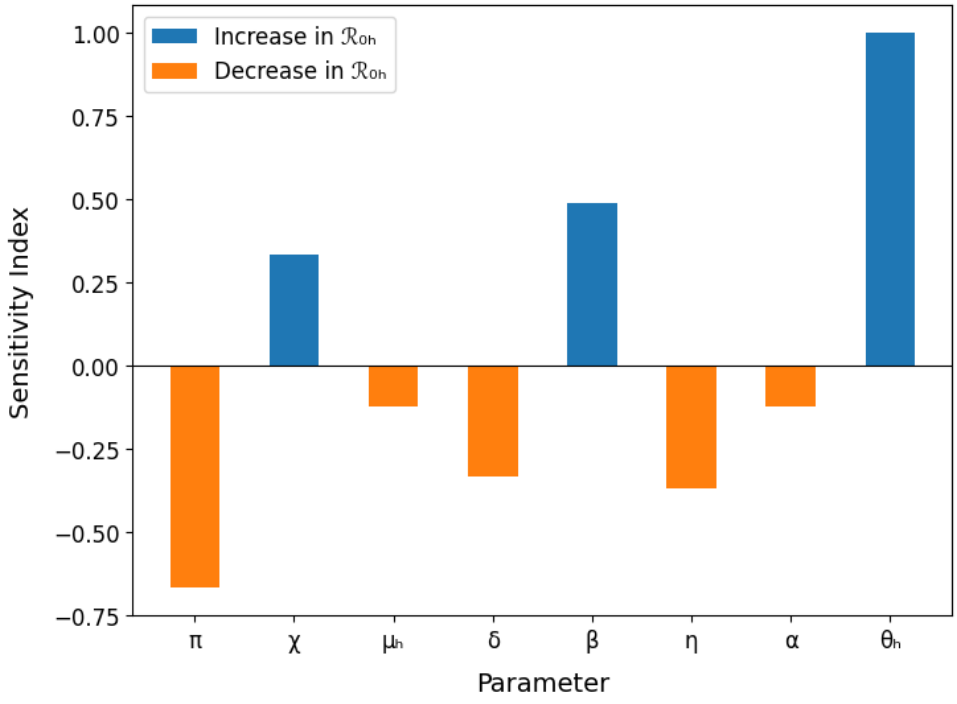

FIGURE 2. Sensitivity indices of model parameters on $\mathfrak{R}_{0h}$

7. RESULTS AND DISCUSSIONS

7.1. Impact of vaccination and effective contact tracing on $\mathfrak{R}_{0h}$. In this section, we analyze the factors influencing $\mathfrak{R}_{0h}$, a key measure of disease transmission dynamics and control strategies. Using contour plots, we explore the relationships between parameters such as human-to-human contact rate (θ_h), vaccination rate (π), effective contact tracing rate (η), and the rate of progression from exposed to infected (β). These plots provide visual insights into the patterns and trends, helping us understand the impact of these factors on monkeypox transmission dynamics.

Figure 3A provides the interaction between the θ_h and π, regarding the impact on $\mathfrak{R}_{0h}$. The plot reveals that as θ_h increases, the value of $\mathfrak{R}_{0h}$ also increases. This indicates that a higher rate of contact between individuals leads to an elevated transmission potential of the disease, resulting in a larger outbreak size. It also demonstrates that when the π, is very low or no vaccination is implemented, the value of $\mathfrak{R}_{0h}$ tends to be higher. This suggests that a lack of vaccination coverage allows the disease to spread more easily within the population, resulting in a higher risk of an epidemic. Interestingly, when θ_h is high and the vaccination rate, π, is also

high, the value of $\mathfrak{R}_{0h}$ can be observed to be less than 1. This implies that a high vaccination rate in the presence of high contact rate can effectively reduce the transmission potential of the disease, potentially leading to disease control and prevention of a major outbreak.

According to Figure 3B, it can be observed that $\mathfrak{R}_{0h}$ increases as β becomes higher and when there is low vaccination coverage. This indicates a higher potential for rapid disease spread in such scenarios. However, for higher values of β, high vaccination coverage keeps $\mathfrak{R}_{0h}$ below the critical threshold of 1, demonstrating the effectiveness of vaccination in controlling monkeypox transmission even with a high rate of progression. Moreover, for lower values of β, $\mathfrak{R}_{0h}$ remains below 1 regardless of vaccination coverage, indicating that a low rate of progression naturally limits monkeypox transmission and can help contain the spread.

Figure 3C shows that higher values of θ_h are associated with an increased $\mathfrak{R}_{0h}$, indicating a greater potential for disease spread through human-to-human interactions. The presence of effective contact tracing plays a crucial role in controlling monkeypox transmission, as demonstrated in Figure 3D, where higher levels of contact tracing effectiveness contribute to a reduction in $\mathfrak{R}_{0h}$. Conversely, when contact tracing is low, $\mathfrak{R}_{0h}$ exhibits a significant increase, emphasizing the critical role of contact tracing measures in controlling disease spread. These findings highlight the importance of robust contact tracing protocols and preventive measures in managing and controlling monkeypox outbreaks.

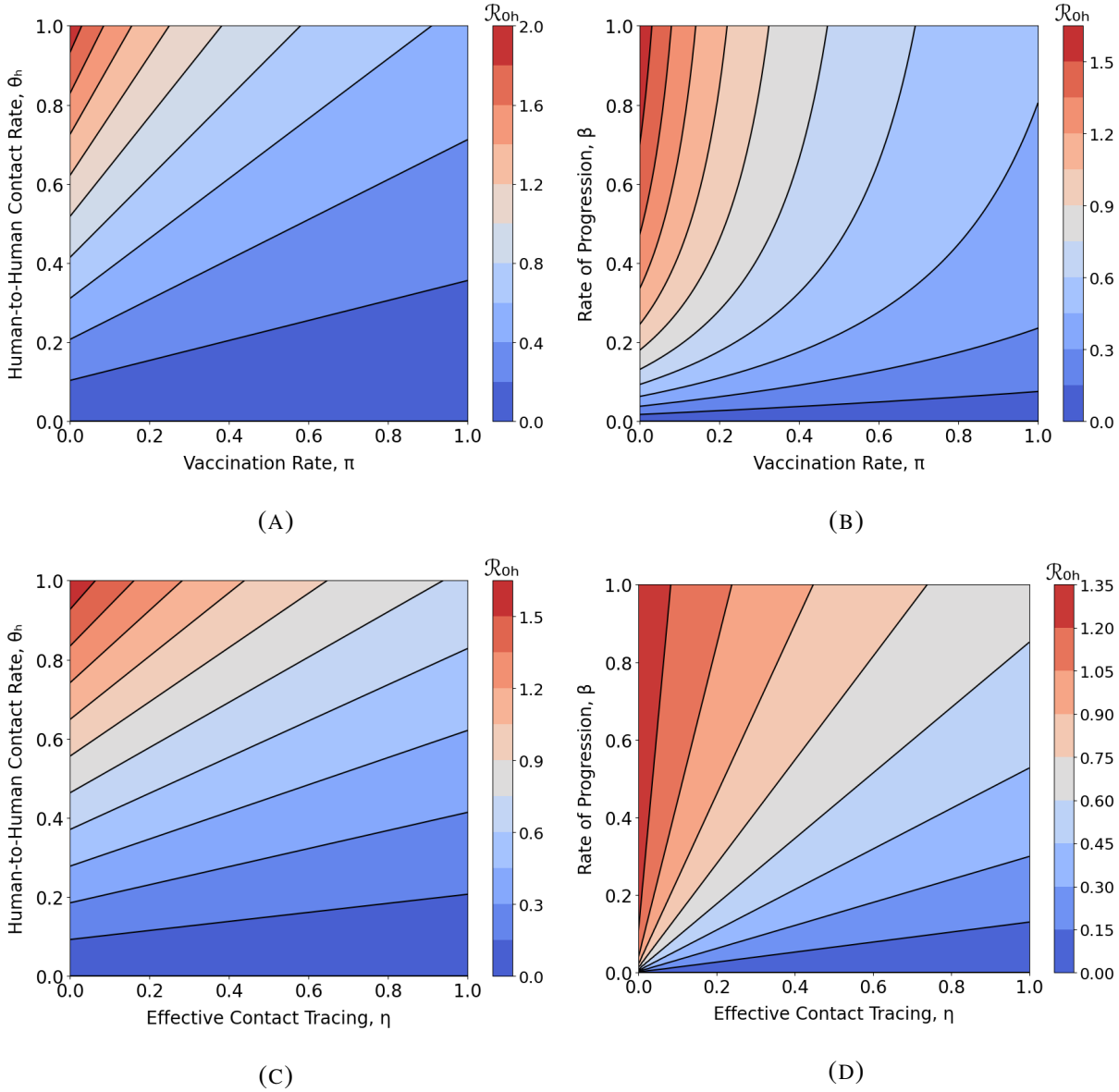

FIGURE 3. Contour plots illustrating the interactions between key parameters and their effects on $\mathfrak{R}_{0h}$. (A) interaction between the human-to-human contact rate and the vaccination rate. (B) interaction between vaccination coverage and the rate of progression from the exposed to the infected state. (C) presents the interaction between the effectiveness of contact tracing and the human-to-human contact rate. Finally, (D) demonstrates the interaction between the effectiveness of contact tracing and the rate of progression from the exposed to the infected state.

7.2. Impact of Vaccination and Effective Contact Tracing on Epidemic Size. In Figure 4, we examined the effect of varying η on the sizes of $E_h(t)$, $Q_h(t)$, $I_h(t)$ and $T_h(t)$. As η increased, we observed a consistent pattern in the sizes of these compartments. Starting with Figure 4A, the size of $E_h(t)$ decreased with increasing η. This indicates that effective contact tracing contributes to the early identification and isolation of individuals who have been exposed to the disease, thereby reducing the number of individuals in the exposed compartment. Figure 4B, on the other hand, demonstrated a tendency for $Q_h(t)$ to grow in size as η grew. This suggests that with better contact tracing, more individuals who have been in close contact with infected individuals are identified and placed under quarantine. Consequently, the quarantined compartment expands as a result of these intensified efforts in isolating potentially infected individuals. In Figure 4C, we observed a reduction in the size of the $I_h(t)$ as η increased. This indicates that more efficient contact tracing leads to a quicker identification and isolation of exposed individuals, limiting their ability to transmit the disease to others. Finally, Figure 4D provides evidence that the size of $T_h(t)$ tends to expand with increasing η. This indicates that as contact tracing becomes more effective, a larger proportion of infected individuals are promptly identified and receive appropriate treatment. As a result, the size of the treated compartment increases, reflecting the positive impact of contact tracing on the timely management of infected individuals.

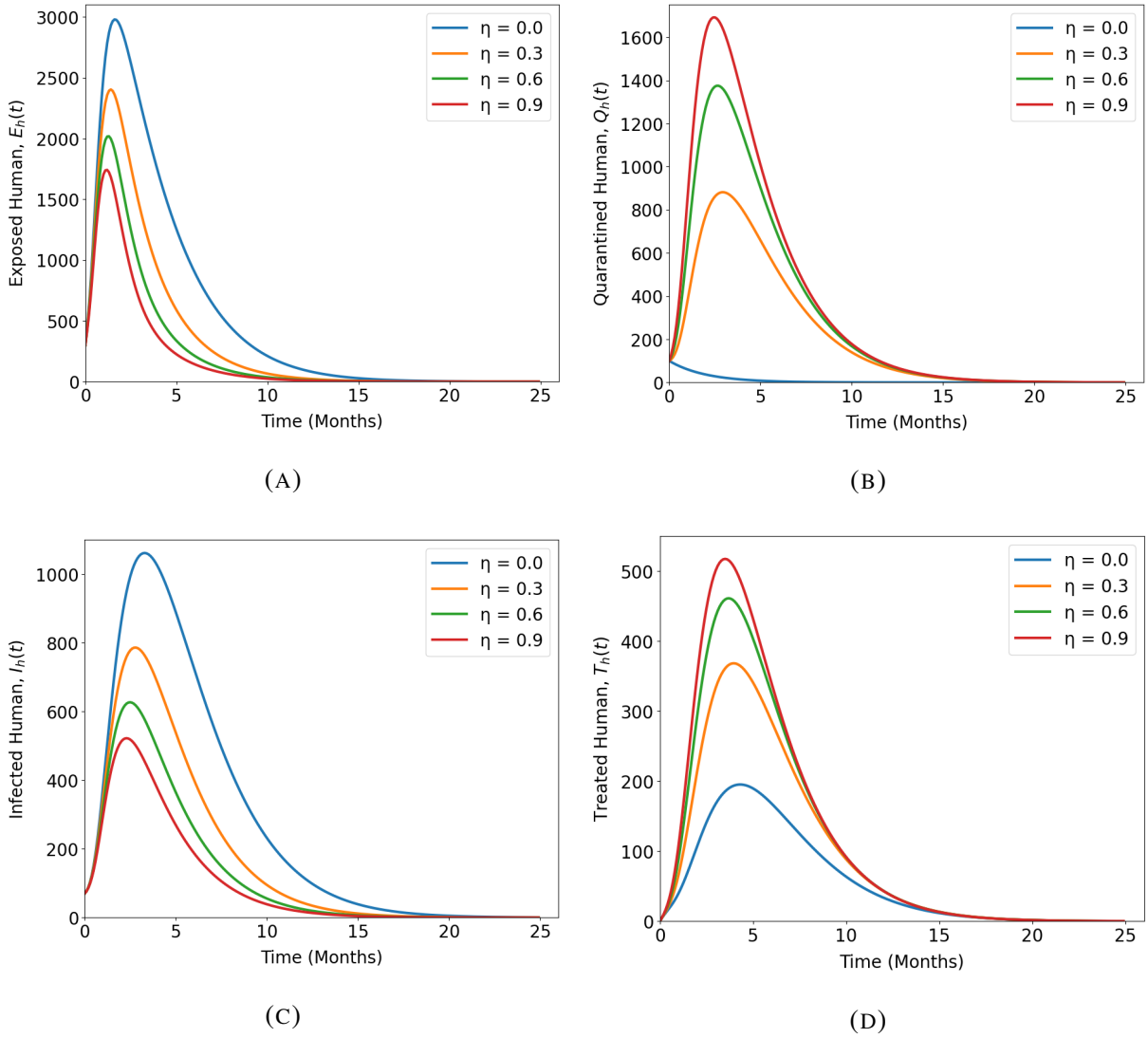

FIGURE 4. The impact of effective contact tracing on $Q_h(t)$, $E_h(t)$, $I_h(t)$ and $T_h(t)$ over time

Aside the contact tracing, we also examined the impact of vaccination on these compartments in Figure 5. By examining the variations in these compartments as π increases, we can assess the influence of vaccination on the transmission dynamics and management of the disease.

In Figure 5A, a consistent decrease in the size of $E_h(t)$ was observed as π increased. This indicates that a higher vaccination rate leads to a reduction in the number of individuals who become exposed to the disease. Vaccination provides protection against infection and lowers the likelihood of individuals transitioning to the Exposed compartment, thus limiting the spread of the disease. This finding suggests that as more individuals are vaccinated, the number of

individuals requiring quarantine due to exposure to infected individuals decreases, as shown in Figure 5B. As the size of the Exposed compartment decreases, there is a subsequent decrease in the number of individuals transitioning to the quarantined compartment. This highlights the effectiveness of vaccination in preventing the progression of exposed individuals to the infectious stage. Similarly, in Figure 5C, an inverse relationship between the vaccination rate and the size of the infected compartment is observed. As the vaccination rate increases, the number of infected individuals decreases, indicating the significant role of vaccination in reducing the spread of the disease. Furthermore, Figure 5D shows a decreasing trend in the treated compartment with higher vaccination rates. When a population is vaccinated against a specific disease, the vaccination aims to provide immunity and prevent individuals from becoming infected or experiencing severe symptoms if they do contract the disease. By reducing the number of infections within the population, vaccination can help prevent the disease from progressing to a severe state, leading to a decreased need for medical interventions, hospitalizations, and treatments.

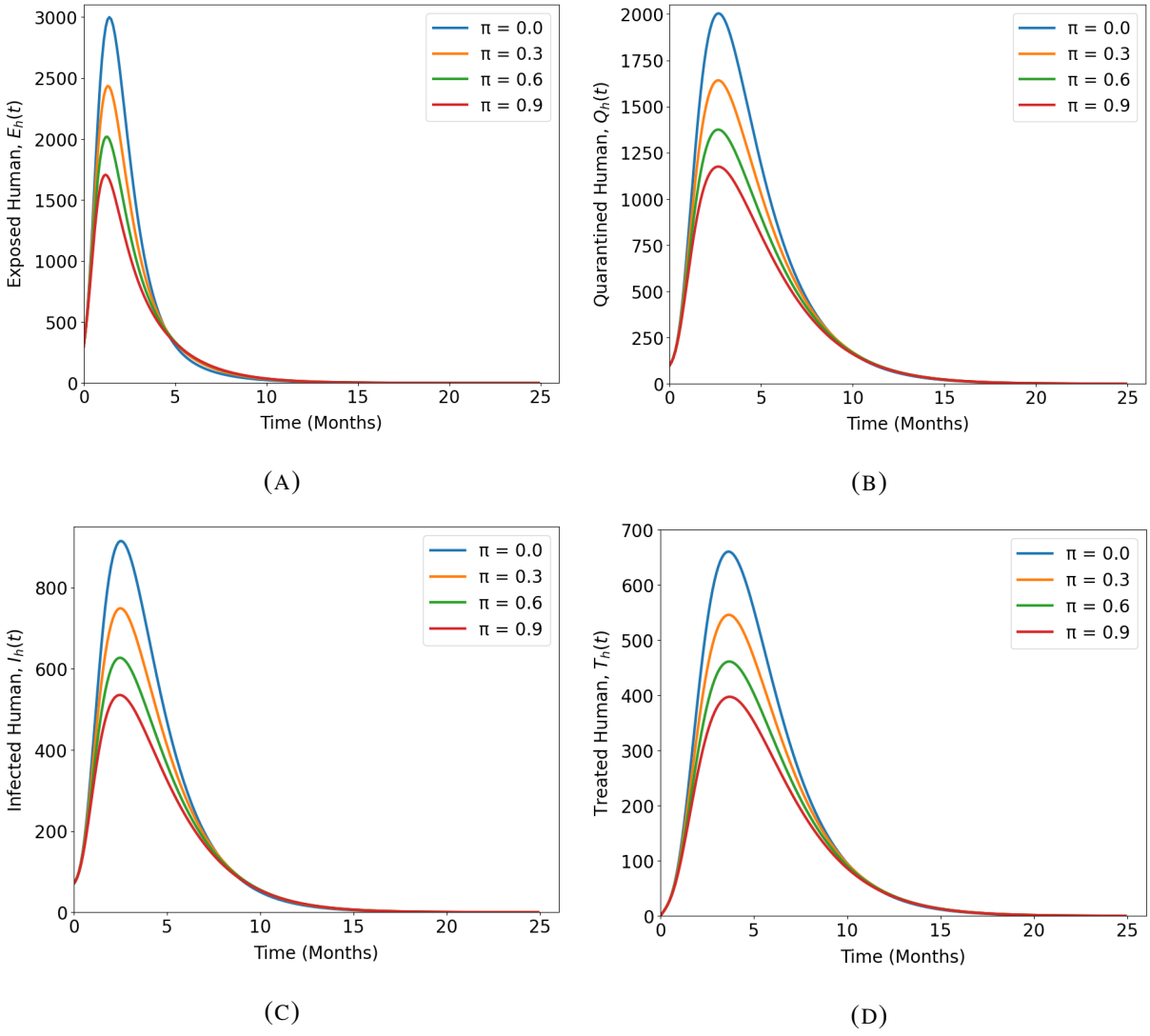

FIGURE 5. The impact of vaccination on the sizes of Q_h, E_h, I_h and T_h over time

8. CONCLUSION

In this study, the dynamics of monkeypox virus transmission were comprehensively examined, with a focus on the prevention and control of the disease's spread through vaccination and efficient contact tracing. The equilibrium points of the model were derived and analyzed to determine the stability of the system. $\mathfrak{R}_0$ was utilized as a threshold parameter. The analysis revealed that when $\mathfrak{R}_0 < 1$, the disease-free equilibrium point is both locally and globally asymptotically stable. This stability criterion implies that, under certain conditions, the disease

can be effectively eradicated from the population. The numerical simulations carried out supported this conclusion by showing that $\mathfrak{R}_0$ can be decreased below unity with effective contact tracing and effective vaccination. The identification and monitoring of people who have had frequent contact with infected people is made possible via contact tracing. The risk of additional transmission is reduced by quickly identifying and isolating these contacts. The execution of preventive measures, such as vaccination or post-exposure prophylaxis, for people who may have been exposed to the virus is also made possible via contact tracing. With this tailored strategy, the disease is further slowed down by ensuring that people who are most at risk of infection receive the appropriate treatments. The thorough analysis provided in this work highlights the symbiotic role that contact tracing and vaccination have in controlling the dynamics of monkeypox transmission. When used together, these strategies significantly contribute to interrupting the transmission chain, thereby stopping the virus's transmission. These findings emphasize the need for continued efforts in promoting vaccination programs and strengthening contact tracing capabilities to effectively manage and contain monkeypox outbreaks.

CONFLICT OF INTERESTS

The author(s) declare that there is no conflict of interests.

REFERENCES

[1] I.D. Ladnyj, P. Ziegler, E. Kima, A human infection caused by monkeypox virus in Basankusu Territory, Democratic Republic of the Congo, Bull. World Health Organ. 46 (1972), 593.

[2] C.P. Bhunu, S. Mushayabasa, Modelling the transmission dynamics of pox-like infections, IAENG Int. J. Appl. Math. 41 (2011), 1-10.

[3] P.V. Magnus, E.K. Andersen, K.B. Petersen, A. Birch-Andersen, A pox-like disease in cynomolgus monkeys, Acta Pathol. Microbiol. Scand. 46 (1959), 156–176.

[4] O.J. Peter, S. Kumar, N. Kumari, et al. Transmission dynamics of monkeypox virus: a mathematical modelling approach, Model Earth Syst. Environ. 8 (2022), 3423–3434.

[5] E. Alakunle, U. Moens, G. Nchinda, et al. Monkeypox virus in Nigeria: infection biology, epidemiology and evolution, Viruses 12 (2020), 1257.

[6] A. Kantele, K. Chickering, O. Vapalahti, et al. Emerging diseases - The monkeypox epidemic in the Democratic Republic of the Congo, Clinical Microbiol. Infect. 22 (2016), 658–659.

[7] P.C. Emeka, M.O. Ounorah, F.Y. Eguda, et al. Mathematical model for monkeypox virus transmission dynamics, Epidemiology 8 (2018), 348.

[8] S. Usman, I.I. Adamu, Modeling the transmission dynamics of the monkeypox virus infection with treatment and vaccination interventions, J. Appl. Math. Phys. 5 (2017), 2335.

[9] C.E. Madubueze, I.O. Onwubuya, G.N. Nkem, et al. The transmission dynamics of the monkeypox virus in the presence of environmental transmission, Front. Appl. Math. Stat. 8 (2022), 2297–4687.

[10] S.V. Bankuru, S. Kossol, W. Hou, et al. A game-theoretic model of monkeypox to assess vaccination strategies, PeerJ 8 (2020), e9272.

[11] R. Grant, L.L. Nguyen, R. Breban, Modelling human-to-human transmission of monkeypox, Bull. World Health Organ. 98 (2020), 638.

[12] V. Capasso, Mathematical structures of epidemic systems, Lecture Notes in Biomathematics, Volume 97, Springer, (1993).

[13] J.K. Asamoah, F.T. Oduro, E. Bonyah, et al. Modelling of rabies transmission dynamics using optimal control analysis, J. Appl. Math. 2017 (2017), 2451237.

[14] S. Busenberg, K. Cooke, Vertically transmitted diseases: models and dynamics, Springer, (2012).

[15] A. Stuart, A.R. Humphries, Dynamical systems and numerical analysis, Cambridge University Press, (1998).

[16] O. Diekmann, J.A.P. Heesterbeek, M.G. Roberts, The construction of next-generation matrices for compartmental epidemic models, J. R. Soc. Interface 7 (2010), 873–885.

[17] C.C. Castillo, Z. Feng, W. Huang, On the computation of $\mathscr{R}_0$ and its role on global stability, in Mathematical approaches for emerging and reemerging infectious diseases: an introduction (Minneapolis, MN, 1999), 229–250, IMA Vol. Math. Appl., 125, Springer, New York.

[18] B. Gbadamosi, M. Ojo, S. Oke, et al. Qualitative analysis of a dengue fever model, Math. Comput. Appl. 23 (2018), 33.

[19] C.M. Veronica, O. Olusegun, A. Newton, et al. Mathematical modeling and stability analyses on the transmission dynamics of bacterial meningitis, J. Math. Comput. Sci. 11 (2021), 7384–7413.

[20] K. Das, G.R. Kumar, K.M. Reddy, et al. Sensitivity and elasticity analysis of novel coronavirus transmission model: a mathematical approach, Sensors Int. 2 (2021), 100088.